A Treatment Combined Prussian Blue Nanoparticles With Low-intensity Pulsed Ultrasound Alleviates Cartilage Damage in Knee Osteoarthritis by Initiating PI3K/Akt/mTOR Pathway

Deyu Zuo
Second affiliated Hospital of Chongqing Medical University
Botao Tan
Second affiliated Hospital of Chongqing Medical University
Gongwei Jia
Second affiliated Hospital of Chongqing Medical University
Dandong Wu
Second affiliated Hospital of Chongqing Medical University
Lehua Yu
Second affiliated Hospital of Chongqing Medical University
Lang Jia (hounsfield@foxmail.com)
Department of Rehabilitation Medicine, The Second Affiliated Hospital of Chongqing Medical University, People's Republic of China

---

Research article

Keywords: osteoarthritis (OA), Prussian blue nanoparticles (PBNPs), Low-intensity pulsed ultrasound (LIPUS)

Posted Date: September 18th, 2020

DOI: https://doi.org/10.21203/rs.3.rs-77010/v1

Abstract

Background: Reactive oxidative stress (ROS) related apoptosis in chondrocytes and extracellular matrix (ECM) degradation play crucial roles in the process of osteoarthritis (OA). Prussian blue nanoparticles (PBNPs) are known to scavenge ROS in cellular. Low-intensity pulsed ultrasound (LIPUS) has been used as a non-invasive modality for the is widely used in clinical rehabilitation management of OA.

Methods: In this study, we aim to investigate the effects of PBNPs/LIPUS combined treatment on knee osteoarthritis (KOA) and to determine whether phosphoinositide 3-kinase (PI3K)/Akt/mammalian target of rapamycin (mTOR) signaling pathway mediates this process. Use LPS to process primary cells of knee joint cartilage to establish a cartilage knee arthritis model. After treated with LIPUS and PBNPs, cell viability was rated by CCK-8 and ROS levels were assessed by DCFH-DA. Cell apoptosis was estimated by flow cytometry and TUNEL staining. Articular pathological changes were observed by naked eyes, H&E, and Safranin O staining, then monitored by cartilage lesion grades and Mankin's score. Protein levels of cleaved caspase-3, Bcl-2, Bax, p-PI3K, PI3K, p-Akt, Akt, p-mTOR, mTOR, IL-1β, MMP3, MMP13, p-JINK, JINK, p-c-Jun, and c-Jun were subjected to western blot.

Results: Cellular ROS, apoptosis rate, and TUNEL staining of chondrocytes were fairly decreased in the PBNPs group and the LIPUS group but drastically down-regulated in the PBNPs/LIPUS combination treatment group when compared with the LPS group. Both PBNPs and LIPUS decreased the grades of cartilage lesions and Mankin scores of knee articular cartilage, while combined administration achieved more reduction. Western blot results showed that the cleaved caspase-3, Bax, IL-1β, MMP3 and MMP13 in the PBNPs and LIPUS groups slightly decreased, and Bcl2 increased slightly, while in the combination treatment group, the former was significantly decreased, and Bcl2 was Significantly increased.

Conclusion: The PBNPs/LIPUS combination treatment increased protein levels of p-PI3K, p-Akt, and p-mTOR but decreased the protein levels of p-JINK and p-c-Jun, *in vitro* and *vivo*. The PBNPs/LIPUS combination treatment reduced cellular ROS, apoptosis, and matrix metalloproteinases (MMPs), as a consequence, alleviated articular cartilage damage in KOA. Moreover, the PBNPs/LIPUS combination treatment suppressed the JINK/c-Jun signal pathway.

Background

Known as degenerative osteoarthritis, OA is the most common disease in the middle-aged and senior population. The pathological characteristics of OA include joint cartilage atrophy, degeneration, bone formation at the joint edge and surface, as well as bone and synovial hyperplasia. At an advanced stage, OA may elicit limited joint function and even paralysis [1, 2]. Articular cartilage is composed of ECM and sparsely distributed chondrocytes. Metabolic and structural changes of articular cartilage namely chondrocyte apoptosis and excessive degradation of ECM play a crucial role in the occurrence and progression of OA [3–6]. In this regard, firstly, the ROS is closely connected with chondrocyte death in OA. Previous studies have reported that "oxidative stress" leads to chondrocyte death and matrix degradation

[7], and ·NO has been considered as a primary inducer of chondrocyte apoptosis [8]. Secondly, MMPs are the most important proteolytic system for the degradation of ECM [9]. During the pathologic process of OA, the degeneration of proteoglycan and type-II collagen are predominantly related to MMP-3 and MMP-13 [10–12].

Current non-surgical therapies for OA contain topical use of non-steroidal anti-inflammatory drugs (NSAIDs), oral medication of NSAIDs or paracetamol, and intra-articular injection of corticosteroids and hyaluronan [13–15]. However, those modalities can cause adverse reactions such as gastrointestinal reactions and osteonecrosis, moreover, they can't reverse the development of OA at the cellular level.

As a clinical application agent with FDA approval, prussian blue (PB) is widely utilized as a dye and an iron staining of biopsy specimens, which arouses extensive attention. Additionally, PB has served in various fields including magnetics, photology, electrochemistry, and biomedicine [16–19]. Recently, it has been reported that PBNPs, with a hollow structure, can effectively scavenge reactive oxygen species in the Institute for Cancer Research of mice, attributing to their affinity for hydroxyl radicals and their ability to simulate three antioxidant enzymes: peroxidase, catalase, and superoxide dismutase [20]. Although PB boasts multiple functions, its therapeutic application in OA by scavenging ROS from chondrocytes and alleviating inflammation has not been verified yet. As a safe and non-invasive biophysical therapy, LIPUS can effectively alleviate swelling and inflammation in animal models of osteoarthritis, thereby delaying the degeneration of articular cartilage and promoting cartilage repair [21–23]. Accumulative studies have indicated that LIPUS influences the differentiation of bone marrow mesenchymal stem cells and promotes chondrogenesis [24–27]. What's more, ultrasound enhances substrate delivery into cells by extracellular uptake of fluid, drugs, and DNA in vitro [28, 29].

The PI3K/Akt/mTOR signaling pathway plays a vital role in regulating cell proliferation, apoptosis, and transformation [30]. Moreover, abundant researches have indicated that the PI3K/Akt/mTOR pathway is involved in OA pathological pathogenesis [31–33].

In this study, we initially utilized PBNPs combined with LIPUS to treat the KOA model *in vitro* and *vivo*, aimed to investigate the effects of LIPUS/PB combination treatment on the ROS, apoptosis, and matrix degradation of articular cartilage with KOA, and figured out whether PI3K/Akt/mTOR signaling pathway mediated the effects of PBNPs/LIPUS combination treatment.

Methods

Synthesis of PBNPs

PBNPs were prepared by adding 495 mg $K_3Fe(CN)_6$ (SCR) and 5 g PVP (K-30, Urchem) to a 40 mL 1M HCL solution, and stirred vigorously until the solution was clarified. It was put at 80℃ for 20 h, centrifuged at 1400 r/min for 15 min and the supernatant was discarded. Then the material was cleaned with double stilled water using an ultrasonic cleaning machine and centrifuged again. The materials were mixed up with 5 mL saline for storage.

Characterization of PBNPs

The particle size and morphology of the PBNPs obtained above were characterized by transmission electron microscopy (TEM, FEI TECNAI G2 F20, FEI, USA), scanning electron microscopy (SEM, FEI Nova Nano 450, FEI, USA) and X-ray diffractometer (PANalytical X'Pert PRO, PANalytical, Holland). Both the average size and the average zeta potential of PBNPs were measured by using a Nano-size potentiometer (Zetasizer Nano ZS90, Malvern, UK).

Cell culture

New Zealand rabbits were purchased from Chongqing Medical University and sacrificed after air injection through the ear vein. The knee articular cartilage was separated under aseptic conditions; the fascia and cartilage membrane of the wrapped cartilage tissue was stripped off and placed in a dish containing PBS solution. The isolated cartilage tissue was cut into blocks of 0.3-0.5 mm, transferred into a 25 cm^2 culture flask and washed with PBS solution containing double antibodies 3 times. 0.25% of trypsin was added at a dosage of 10-15 times the volume of cartilage, and digestion was terminated after being treated at 37°C for 1-2 h. Cartilage tissue was incubated with 0.02% type II collagenase at 37°C overnight. Cells were observed using an inverted microscope. In the absence of single cells, DMEM medium was added to dilute the type II collagenase to terminate digestion. The cell mass was blown into a single cell and then filtered with a 200 mesh sieve to collect the filtrated. Next, the filtrated was centrifuged at 1500 r/min for 5 min. After that, the supernatant was discarded, and cells were cultured with DS medium at 37℃ with 5% CO_2. All the animals were euthanatized according to the standards of the Ethics Committee of Chongqing Medical University.

Animals

Twenty-five male New Zealand rabbits (11 months old, 3.0-3.5 kg) were obtained from Chongqing Medical University and housed in individual cages with a cycle of 12 h of light and 12 h of darkness at 20-25℃. To construct the KOA model, the anterior cruciate ligament was transected from the right knee of 20 rabbits under general anesthesia (3% pentobarbital, 1 mL/kg) by using ophthalmic scissors as previously described [34]. The other 5 rabbits served as controls. After postoperative wk 1, rabbits were induced to move for 30 min daily for 5 d per wk for 7 wk to promote OA development.

After 4 wk of OA induction [35], 20 rabbits with KOA were randomly divided into 4 groups including KOA (n=5), KOA+PBNPs (120 μg/mL article injection once a week for 6 weeks, n=5), KOA+LIPUS (n=5) and KOA+PBNPs combined with LIPUS (n=5) groups. Rabbits in all groups were sacrificed by air embolization at 6 wk after each intervention. All experiments were approved by the Animal Management Rule of the Chinese Ministry of Health and the Chongqing Medical University Animal Ethics Committee.

Macroscopic observation

The femoral condyle articular cartilages from knee joints were collected 6 wk after ACLT and observed by naked eyes. The criterion of cartilage injury grading was referred to as Outerbridge's grading standard [36] (**Table 1**).

Histopathology

After general observation, the specimens were fixed with neutral formalin and processed for histopathologic examination. The samples were decalcified in ethylenediaminetetraacetic acid for 3 wk, embedded in paraffin, and sliced into 4 μm sections using a microtome for microscopic examination. Pathologic changes of knee joint cartilage specimens were observed under a microscope, including surface irregularity, crack formation, and decrease of Safranin O staining of articular cartilage. Modified Mankin scoring scale (**Table 2**) was used to evaluate fibrosis, matrix distribution, cartilage loss, and chondrocyte colonization. Microscopic evaluations were performed by two independent experts in a double-blind fashion.

LIPUS stimulation

LIPUS (Osteotron Ⅱ, ITO Physiotherapy&Rehabilitation) was applied to chondrocytes and rabbits with KOA. LIPUS (acoustic intensities of 30 mW/cm^2, 45 mW/cm^2 and 60 mW/cm^2, duty ratio 40%, central frequency 1.5 MHz, repetition frequency 1 kHz and operating time 20 min per day) was applied to the chondrocytes after being cultured 24 h at the bottom of the culture dish.

As for the rabbits with KOA, LIPUS was administrated to the right knee as follows: acoustic intensities of 60 mW/cm^2, a duty ratio of 20%, central frequency of 1.5 MHz, repetition frequency of 1 kHz, the irradiation time of 20 min per day, and 5 days per week for 6 wk. The process was standardized with a device that the rabbits were placed in a supine position with the knee angled approximately 120 at the flexion position. The ultrasound probe was attached to the skin of the medial femoral condyle, and the target tissue was cartilage of the medial femoral condyle.

Cell death assessment

The effects of PBNPs on cartilage cell death were determined by Cell Counting Kit-8 (CCK-8) colorimetric assay (Sigma, USA). Briefly, podocytes were seeded into 96-well plates at a density of 10^4 cells per well and cultured in complete RPMI-1640 culture medium for 24 h. Then, the cells were treated with PBNPs at a concentration of 0, 30, 60, 120, 150, and 180 μg/mL respectively for 24 h and 120 μg/mL for 1, 2, 3, 4, 5, 6 and 7 days. CCK8 was added to each well and the cells were incubated at 37°C with 5% CO_2 for 2 h. Absorbance was quantified at 450 nm using a multi-well fluorescent plate reader (Thermo Scientific Varioskan Flash, Thermo Fisher Scientific, USA). The rate of cell death was calculated.

Flow cytometric analysis

The treated cells were collected by centrifugation at 1000 r/min for 3 min, washed twice with ice-cold PBS, gently resuspended in 500 μL 1×Annexin V binding buffer containing 5 μL Annexin V-FITC and 3 μL

of PI before being incubated at room temperature in the dark for 10 min. The percentage of apoptotic cells was analyzed by flow cytometry (BD FACSCalibur, Becton-Dickinson, USA).

Tunel staining

Cell apoptosis was determined using the One-Step TdT-mediated dUTP Nick-End Labeling (TUNEL) Apoptosis Assay Kit (Beyotime, China). Pretreated cells in 12-well plates were washed twice with PBS, incubated with 50 μL TUNEL testing solution at 37℃ for 1 h in the dark, and then washed with PBS 3 times. After the membrane was sealed with anti-fluorescence quenching solution, the cells were observed at an excitation wavelength of 550 nm and the emission wavelength of 570 nm using a fluorescence microscope (Zeiss Fluorescence Microscope, Germany).

ROS detection

The pretreated cells in 12-well plates were incubated with 2', 7-dichlorofluorescein diacetate (DCFH-DA) (10 μmol/L) at 37°C for 30 min and washed with PBS. The cell fluorescence was observed by using a fluorescence microscope (Zeiss Fluorescence Microscope, Germany) at an excitation wavelength of 488 nm and an emission wavelength of 525 nm.

Western blot analysis

Proteins extracted from cartilage cells were collected after treatment. The cells were lysed with RIPA (Beyotime, China) and PMSF, sonicated (noise-isolating tamber, Ningbo Scientz Biotechnology Co., Ltd.) for 12 s (20% power, 1-s pulse on, and 2-s pulse off), and centrifuged at 12,000 g for 15 min at 4℃. Protein concentrations were quantified with the BCA Protein Assay Kit (Beyotime, China). An equal volume of protein samples was loaded per lane and electrophoretically transferred onto PVDF membranes (Millipore, USA). The membranes were blocked in 5% skimmed milk for 1.5 h at room temperature and incubated with different primary antibodies: rabbit anti-cleaved caspase-3 (CST, USA), rabbit anti-Bcl2 (1:1000, CST, USA), rabbit anti-Bax (1:1000, CST, USA), rabbit anti-p-PI3K (1:1000, CST, USA), rabbit anti-PI3K (1:1000, CST, USA), rabbit anti-p-Akt (1:1000, CST, USA), rabbit anti-Akt (1:1000, CST, USA), rabbit anti-p-mTOR (1:1000, CST, USA), rabbit anti-mTOR (1:1000, CST, USA), rabbit anti-IL-1β (1:1000, Proteintech, USA), rabbit anti-MMP3 (1:1000, CST, USA), rabbit anti-MMP13 (1:1000, CST, USA), rabbit anti-p-JINK (1:1000, CST, USA), rabbit anti-JINK (1:1000, CST, USA), rabbit anti-p-c-Jun (1:1000, CST, USA), rabbit anti-c-Jun (1:1000, CST, USA), and β-actin (1:5000, Sungene Biotech, China) overnight at 4°C. After being washed with TBS-T, the membranes were incubated either with goat anti-mouse IgG (H+L) horseradish peroxidase (1:8000, MultiSciences, China) or goat anti-rabbit IgG (H+L) horseradish peroxidase (1:8000, MultiSciences, China) for 1 h at room temperature and incubated with ECL reagent (Advansta, USA). Protein blot images were captured using an ECL chemiluminescence system (GE Healthcare, Piscataway, NJ, USA) and quantified with Quantity One software.

Statistical analysis

Data were presented as mean±SD from 3 independent experiments. Analyses were carried out by using GraphPad Prism Software version 6.00 (San Diego, CA). The data complied with normal distribution and homogeneity of variance. Statistical comparisons between the two groups were analyzed using the two-tailed unpaired Student's t-test. Differences among multiple groups were analyzed using a one-way analysis of variance (ANOVA) followed by Tukey's t-test. The value of P less than 0.05 was considered statistically significant.

Results

Characterization of PBNPs

The PBNPs were prepared by using simple colloidal chemistry with polyvinylpyrrolidone (PVP), which is a universal auxiliary material in pharmaceuticals as a stabilizer. The morphology of PBNPs was observed by using scanning electron microscopy (SEM) (**Fig. 1A**) and transmission electron microscopy (TEM) (**Fig. 1B**). The synthesized PBNPs were cubic particles with an average size of about 80.06 nm (**Fig. 1C**) and the average zeta potential of PBNPs was about -15.1 mv (**Fig. 1D**). The single-crystal structure was confirmed by electron diffraction of the whole particle of PBNPs (**Fig. 1E**).

The cell viability assay was performed with different concentrations of PBNPs, and no significant difference was revealed between the groups of 30 μg/mL, 60 μg/mL, and 120 μg/mL and the control group (incubated with normal saline). Conversely, a remarkable decrease in the cell viability was exhibited in the groups of 150 μg/mL and 180 μg/mL (**Fig. 1F**). Moreover, no significant difference was shown from day 1 to day 7 when the cells were treated with 120 μg/mL PBNPs at a different time (**Fig. 1G**).

Effects of PBNPs/LIPUS treatment on the ROS induced by LPS in chondrocytes

To investigate effects of PBNPs/LIPUS treatment on ROS production in chondrocytes, cells were pretreated with 1 μg/mL LPS and handled with various concentrations (30 μg/mL, 60 μg/mL and 120 μg/mL) of PBNPs as well as various acoustic intensities (30 mW/cm^2, 45 mW/cm^2 and 60 mW/cm^2) of LIPUS for 7 d. ROS production was estimated by using a fluorescent probe DCFH-DA. As shown in **Fig. 2A**, the ROS production in cells treated with LPS was much higher than that in the control, and PBNPs reduced the LPS-induced ROS production in a dose-dependent manner. In addition, LIPUS treatment also alleviated LPS-induced ROS as the intensity increased (**Fig. 2B**). To further determine the effects of PBNPs/LIPUS combined treatment on LPS-induced ROS in chondrocytes, we treated cells with 120 μg/mL of PBNPs, 60 mW/cm^2 of LIPUS and a combination of both in severally. As a result, an evident reduction of ROS was observed in cells of the combination treatment group when compared with the PBNPs and the LIPUS group (**Fig. 2C**). These data indicated that the combined treatment could eliminate LPS-induced ROS better than the treatment of either PBNPs or LIPUS.

Effects of PBNPs/LIPUS treatment on apoptosis induced by LPS in chondrocytes

The effects of PBNPs/LIPUS treatment on apoptosis in chondrocytes were examined with flow cytometry assay and TUNEL staining. A substantial increase of apoptosis in the cells treated with LPS was observed compared with the control, yet PBNPs dose-dependently reduced apoptosis of chondrocytes induced by LPS (**Fig. 3A and 3B**). Similarly, LIPUS treatment alleviated the apoptosis induced by LPS in reverse trends of increasing acoustic intensity (**Fig. 3C and 3D**). Next, we combined PBNPs with LIPUS and found that the PBNPs/LIPUS combination treatment inhibited the apoptosis induced by LPS more effectively than either PBNPs or LIPUS alone (**Fig. 4A and 4B**). We further detected the expression of the apoptosis-related proteins by using western blot. As shown in **Fig. 4C**, Bax, and cleaved caspase-3, which played a critical role in the regulation of cell apoptosis, were notably up-regulated in cells treated with LPS compared with the control. A radical reduction of Bax and cleaved caspase-3 was observed in the groups of PBNPs, LIPUS, and the combination treatment when compared with the LPS group. The protein expression of the combination treatment group was significantly reduced when compared with either the PBNPs or the LIPUS. Correspondingly, the antiapoptotic protein Bcl2 was signally reduced in the LPS group when compared with the control group. All the therapies with PBNPs, LIPUS, and the combination of both revealed an increase of Bcl2 expression compared with the LPS group, whereas the combined treatment promoted Bcl2 expression more efficiently in contrast to the single administration of either PBNPs or LIPUS. The findings indicated that the combined treatment could alleviate LPS-induced apoptosis better than the single treatment of either PBNPs or LIPUS.

PBNPs/LIPUS treatment initiated the PI3K-Akt-mTOR pathway to reduce the LPS-induced ROS and apoptosis in chondrocytes

To determine the mechanism of PBNPs/LIPUS treatment reducing the LPS-induced ROS and apoptosis in chondrocytes, the protein expressions of p-PI3K, PI3K, p-Akt, Akt, p-mTOR, and mTOR were severally detected by western blot. Compared with the control, the protein levels of p-PI3K, p-Akt, p-mTOR revealed an intense diminish in the LPS-treated chondrocytes. However, combined treatment significantly increased the expression of p-PI3K, p-Akt, and p-mTOR compared with the LPS group (**Fig. 5A**), which indicated that PBNPs/LIPUS combined treatment initiated the PI3K-Akt-mTOR pathway. To further determine whether the PI3K-Akt-mTOR pathway mediates the effects of PBNPs/LIPUS combined treatment on ROS and apoptosis in chondrocytes, we pretreated cells with 100 nmol/L of wortmanin, and an inhibitor of PI3K. As a result has shown, wortmanin noticeably reduced the levels of p-PI3K, p-Akt, and p-mTOR in the cells with combined treatment (**Fig. 5B**). Additionally, PI3K inhibition sharply increased the ROS that was originally reduced by the combination therapy (**Fig. 5C**). Furthermore, a considerable increase in apoptosis was observed through flow cytometry assay and TUNEL staining after PI3K inhibition (**Fig. 5D and 5E**). Also, the expression of Bax and cleaved caspase-3 in the combined treatment group were significantly increased after a wortmanin addition, while Bcl2 was notably reduced (**Fig. 5F**). These data indicated that PBNPs/LIPUS combination treatment reduced the LPS-induced ROS and apoptosis in chondrocytes by initiating the PI3K-Akt-mTOR pathway.

PBNPs/LIPUS treatment inhibited IL-1β and MMPs while activated JINK/c-Jun signal pathway in LPS-incubated chondrocytes

As results have shown, the IL-β, MMP3, and MMP13 protein expressions were dramatically elevated in LPS-incubated cells when compared with the control, whereas a prominent reduction was displayed in the groups of PBNPs, LIPUS, and the combined treatment when compared with the LPS group. There was also an evident decrease in the PBNPs/LIPUS combined treatment in contrast to either the PBNPs or LIPUS (**Fig. 6A and 6B**). These data revealed that PBNPs/LIPUS combined treatment could directly inhibit the inflammation and degeneration of ECM in chondrocytes. Furthermore, the p-JINK, JINK, p-c-Jun (ser308), and c-Jun protein expressions were detected. Compared with the control, expressions of p-JINK and p-c-Jun protein were significantly increased in LPS-treated cells. The protein expressions were largely reduced in the PBNPs/LIPUS combined treatment group in contrast to the LPS group (**Fig. 6C and 6D**). It was, therefore, suggested that combined PBNPs/LIPUS therapy might diminish the inflammation and MMPs in LPS induced chondrocytes through the JINK/c-Jun signal pathway.

Effects of LIPUS/PBNPs treatment on article cartilage in rabbits with KOA

Six weeks after the intervention, macroscopic observation of the femoral condylar cartilage samples in the five groups was exhibited in **Fig. 7A**. In the KOA, severe hypertrophy, whiteness, and softness of articular cartilage with subchondral bone exposure were shown. Moreover, moderate hypertrophy, whiteness, and softness of articular cartilage were observed both in the KOA+PBNPs group and the KOA+LIPUS group. In the KOA+PBNPs+LIPUS group, the surface of articular cartilage was slightly pale and soft. Cartilage lesion grades measured by microscopic examination were shown in **Table 3**. Then the cartilage specimen was stained with hematoxylin and Safranin O was then examined under a microscope. The observations were shown in **Fig. 7B and 7C**. We found the articular cartilage surface was smooth and evenly stained with chondrocytes arranged in normal order in the control. Oppositely, the significant articular cartilage fissures, the apparent loss of staining extending from the surface to the depth as well as the reduction of the number of chondrocytes were observed in the KOA group. In the KOA+PBNPs and the KOA+LIPUS group, we observed moderate surface cracks in the articular cartilage with a medium loss of staining and chondrocytes. We then found minor surface cracks in the articular cartilage with mild loss of staining in the KOA+PBNPs+LIPUS group, and the chondrocytes showed slightly abnormal arrangement with decreased superficial cells. The Mankin scores after 6 wk of treatment were summarized in **Table 4**. As compared with the control group, the total scores were increased in the KOA. Additionally, both total scores in the KOA+PBNPs and the KOA+LIPUS were moderately lower than that in the KOA; however, scores of the KOA with combination treatment was lower than that in the KOA+PBNPs and the KOA+LIPUS respectively. Specifically, when compared with the KOA, the PBNPs treatment mildly reduced the scores in subgroups 1 and 2, and the LIPUS treatment slightly reduced the scores in subgroups 2 and 3. Moreover, the combination treatment significantly decreased the scores in subgroup 1, 2, and 3 in contrast with the KOA.

Additionally, protein expressions of articular cartilage were detected by western blot (**Fig. 8A**). There was a moderate decrease of Bax, cleaved caspase-3, IL-1β, MMP3, and MMP13 and a moderate increase of Bcl2 after PBNPs treatment and LIPUS treatment. Furthermore, the regulation of combination treatment on these proteins manifested more apparently. These data indicated that PBNPs/LIPUS combined

treatment efficiently inhibited the apoptosis of chondrocytes and the ECM damage in knee articular cartilage. Consistent with the result *in vitro*, PBNPs/LIPUS combined treatment activated the PI3K/Akt/mTOR signal pathway and suppressed the JINK/c-JUN axis as well (**Fig. 8B**).

Discussion

Currently, neither surgical nor non-surgical option can reverse the progress of OA on clinical treatment. In this study, we found that the protective effect of PBNPs/LIPUS combined treatment on KOA manifested as suppressing ROS and apoptosis in chondrocytes, which was mediated by PI3K/Akt/mTOR pathway initiation. Besides, the combined treatment also reduced inflammation and expression of MMPs through the suppressed JINK/c-Jun axis. This study was a novel description, and the results partly provided fundamental evidence for the clinical application of PBNPs/LIPUS combination therapy.

Chondrocyte apoptosis was correlated with the severity of cartilage degradation in OA [37]. Despite moderate levels of ROS played an important role in regulating normal chondrocytic activities including cell activation, proliferation, and matrix remodeling [7], a substantial number of researches suggested that ROS was the major cause of OA development [5, 38–40]. Excessive ROS could elicit protein oxidation, lipid peroxidation, and DNA damage resulting in cell damage and apoptosis [41–43]. This study demonstrated that all therapies with LIPUS, PBNPs, and combined PBNPs/LIPUS inhibited ROS in the LPS-treated chondrocytes and decreased apoptosis *in vitro* and *vivo* by up-regulating Bax and cleaved caspase-3 while down-regulating Bcl-2. It has been demonstrated that both PBNPs and LIPUS could scavenge ROS in cellular [20, 44]. Consistent with previous studies, PBNPs and LIPUS reduced the ROS of LPS-pretreated chondrocytes in a dose-dependent and acoustic intensity-dependent manner. Of note, it was initially found that PBNPs (120 μg/mL) and LIPUS (60 mW/cm^2) could alleviate the apoptosis in chondrocytes and cartilage tissue. The anti-apoptotic effects of PBNPs have been rarely reported. Hollow Prussian blue nanozymes (HPBZs) possessed multienzyme activity assisted with $Bi3^+$ and exerted anti-apoptotic effects to protect cells from ischemia-induced injury by regulating the expression of anti- and pro-apoptotic proteins *in vitro* and *vivo* in a recent study [45]. Although the material structure of HPBZs did a little differ from PBNPs, the anti-apoptotic effects may be closely related to ROS scavenging. Nevertheless, the effects of LIPUS on apoptosis are controversial. Focused low-intensity pulsed ultrasound (FLIPUS) affected ECM production in KOA rabbits by decreasing chondrocyte apoptosis [46]. Conversely, LIPUS treatment promoted apoptosis and decreased the viability of endothelial cells, osteoclasts, and preadipocytes in human [47–49]. The opposite results may attribute to different parameters of LIPUS and different cells. We also found that fibrosis, matrix distribution, cartilage loss, and chondrocyte colonization were improved after the PBNPs/LIPUS treatment through macroscopic observation, HE, and Safranin O staining semi quantitated by using cartilage lesion grades and Mankin scores. Excitedly, the PBNPs/LIPUS combination treatment functioned as the most effective one in blocking apoptosis and ROS, thereby promoting cartilage damage recovery. In previous researches, LIPUS has been indicated a role in inducing greater internalization of nanomaterials into cells instead of

affecting their viability [50, 51]. Therefore, PBNPs entered cells more easily assisted with the mechanical function of LIPUS, achieving more powerful anti-apoptotic and ROS clearance effects.

The activation of the PI3K/Akt/mTOR signal pathway is widely recognized as a protective factor in OA. Ginsenoside Rg1 protected chondrocytes from IL-1β-induced mitochondria-activated apoptosis through the PI3K/Akt pathway [33]. The Akt activity enhancement by morroniside could be beneficial to chondrocyte survival [52]. Consistently, we found that PBNPs/LIPUS combination treatment activated PI3K/Akt/mTOR pathway *in vitro* and *vivo*, and PI3K inhibition by using wortmannin reduced the anti-apoptotic and ROS clearance capability of the combination treatment.

It is believed that IL-1β and MMPs could act as possible markers of OA [53, 54]. IL-1β was considered as one of the pro-inflammatory cytokines and highly associated with inflammatory pain [55, 56]. In the pathological process of OA, the up-regulation of MMPs induced by IL-1β especially MMP-1 and − 13, presented as a key event during the irreversible changes of cartilage matrix degradation, for the reason that the type II collagen degeneration and the matrix proteoglycan consequent were released from the cartilage [57, 58]. In previous studies, LIPUS has been demonstrated to decrease MMP's level in OA [59, 60]. In this study, we illustrated that in LPS-treated chondrocytes, protein levels of IL-1β, MMP3, and MMP13 were mildly reduced in the LIPUS treatment group as well as the PBNPs treatment group, while those were significantly decreased in the combination treatment group, both *in vitro* and *vivo*. It has been demonstrated that PBNPs could dramatically reduce the LPS-induced expressions of ALT, IL-6, and IL-8 in serum [20], consistent with the anti-inflammation of PBNPs shown in our study. p38 and JNK enzymes involved in the MAPK pathway played a crucial role in the high-level MMPs expression in arthritic joints because a tightly regulated signaling pathway cascade activation was initiated by inflammatory cytokines namely IL-1β [11, 61]. Our results also showed that JINK/c-Jun were activated by LPS whereas suppressed by the PBNPs/LIPUS combination treatment. Therefore, we assumed that the PBNPs/LIPUS combined treatment might reduce the levels of MMP3 and MMP13 by inhibiting the MAPK pathway, yet its mechanism remains to be explored.

Conclusion

In conclusion, our present study showed that combined PBNPs/LIPUS treatment, which was superior to either PBNPs or LIPUS in articular cartilage protection, could alleviate ROS and apoptosis of chondrocytes by activating the PI3K/Akt/mTOR pathway, reduce inflammatory cytokines and inhibit ECM degradation by reducing MMPs expression. Further studies are required to determine the effects of PBNPs/LIPUS treatment in the clinic.

List Of Abbreviations

Not applicable.

Declarations

Ethics approval and consent to participate

All experiments were approved by the Animal Management Rule of the Chinese Ministry of Health and the Chongqing Medical University Animal Ethics Committee.

Consent for publication

Not applicable.

Availability of data and material

All data generated or analysed during this study are included in this published article.

Competing interests

The authors declare that they have no competing interests.

Funding

This study was supported in part by National Natural Science Foundation of China (Youth Science Fund Project) (Grant No. 81802234), a medical research program of Chongqing Health and Family Planning Commission (Grant No. 2017msxm034), and by science and health joint science and technology project of traditional Chinese Medicine of Chongqing Health and Family Planning Commission and Chongqing Science and Technology Commission (Grant No. zy201802104). The above funding agencies are not involved in the research, collection, analysis and interpretation of data and manuscript writing, only providing financial support.

Authors' contributions

Lehua Yu and Lang Jia analyzed and interpreted the data. Deyu Zuo, Botao Tan, Gongwei Jia and Dandong Wu performed the anminal experiment, Deyu Zuo, Lehua Yu and Lang Jia was a major contributor in writing the manuscript. All authors read and approved the final manuscript.

Acknowledgements

We would like to acknowledge the staff of the Institute of Ultrasound Imaging of Chongqing Medical University and the Ministry of Science and Technology for their technical assistance.

References

1. Brown JP, Boulay LJ. Clinical experience with duloxetine in the management of chronic musculoskeletal pain. A focus on osteoarthritis of the knee. Ther Adv Musculoskelet Dis. 2013;5(6):291-304.

2. Kluzek S, Newton JL, Arden NK. Is osteoarthritis a metabolic disorder? Br Med Bull. 2015;115(1):111-21.
3. Blanco FJ GR, Vasquez-Martul E, de Torro FJ, Galdo F. Osteoarthritis chondrocyte die by apoptosis: a possible pathway for osteoarthritis pathology. Arthritis Rheum. 1998:41:284–9.
4. Horton WE Jr FL, Adam C. . Chondrocyte apoptosis in development, ageing and disease. Matrix Biol 1998:17:107–15.
5. Henrotin YE, Bruckner P, Pujol JPL. The role of reactive oxygen species in homeostasis and degradation of cartilage. Osteoarthritis and Cartilage. 2003;11(10):747-55.
6. Hashimoto S TK, Amiel D, Coutts RGD, Lotz M CHONDROCYTE APOPTOSIS AND NITRIC OXIDE PRODUCTION DURING EXPERIMENTALLY INDUCED OSTEOARTHRITIS Arthritis Rheum. 1998:41:1266–74.
7. Henrotin Y, Kurz B, Aigner T. Oxygen and reactive oxygen species in cartilage degradation: friends or foes? Osteoarthritis Cartilage. 2005;13(8):643-54.
8. Blanco FJ OR, Schwarz RL, Lotz M. Chondrocyte Apoptosis Induced by Nitric Oxide. Am J Pathol 1995:146:75–85.
9. Takaishi H, Kimura, T., Dalal, S., Okada, Y., & D'Armiento, J. Joint diseases and matrix metalloproteinases: A role for MMP-13. Current Pharmaceutical BiotechnologyX. 2008:9.
10. Billinghurst RC, Dahlberg L, Ionescu M, Reiner A, Bourne R, Rorabeck C, et al. Enhanced cleavage of type II collagen by collagenases in osteoarthritic articular cartilage. J Clin Invest. 1997;99(7):1534-45.
11. Mengshol JA, Vincenti, M. P., Coon, C. I., Barchowsky, A., & Brinckerhoff, C. E. Interleukin-1 induction of collagenase 3 (matrix metalloproteinase 13) gene expression in chondrocytes requires p38, c-Jun N-terminal kinase, and nuclear factor kappaB: Differential regulation of collagenase 1 and collagenase 3. Arthritis and Rheumatism. 2000:43, 801–11.
12. Dahlberg L, Billinghurst, R. C., Manner, P. Selective enhancement of collagenase-mediated cleavage of res ident type II collagen in cultured osteoarthritic cartilage and arrest with a synthetic inhibitor that spares collagenase 1 (matrixmetalloproteinase 1). Arthritis and Rheumatism. 2000:43, 673–82.
13. LR E, H C, CL D, TA W, KA H. Future nanomedicine for the diagnosis and treatment of osteoarthritis. Nanomedicine (Lond). 2014:9(14):2203-15. .
14. Qvist P, Bay-Jensen AC, Christiansen C, Dam EB, Pastoureau P, Karsdal MA. The disease modifying osteoarthritis drug (DMOAD): Is it in the horizon? Pharmacol Res. 2008;58(1):1-7.
15. Steinecker-Frohnwieser B, Weigl L, Kullich W, Lohberger B. The disease modifying osteoarthritis drug diacerein is able to antagonize pro inflammatory state of chondrocytes under mild mechanical stimuli. Osteoarthritis Cartilage. 2014;22(7):1044-52.
16. Yang F, Hu S, Zhang Y, Cai X, Huang Y, Wang F, et al. A hydrogen peroxide-responsive O(2) nanogenerator for ultrasound and magnetic-resonance dual modality imaging. Adv Mater. 2012;24(38):5205-11.

17. Jing L, Liang X, Deng Z, Feng S, Li X, Huang M, et al. Prussian blue coated gold nanoparticles for simultaneous photoacoustic/CT bimodal imaging and photothermal ablation of cancer. Biomaterials. 2014;35(22):5814-21.
18. Larionova J, Guari Y, Sangregorio C, Guérin C. Cyano-bridged coordination polymer nanoparticles. New Journal of Chemistry. 2009;33(6).
19. Su L, Xiong Y, Yang H, Zhang P, Ye F. Prussian blue nanoparticles encapsulated inside a metal–organic framework via in situ growth as promising peroxidase mimetics for enzyme inhibitor screening. Journal of Materials Chemistry B. 2016;4(1):128-34.
20. Zhang W, Hu S, Yin JJ, He W, Lu W, Ma M, et al. Prussian Blue Nanoparticles as Multienzyme Mimetics and Reactive Oxygen Species Scavengers. J Am Chem Soc. 2016;138(18):5860-5.
21. Gurkan I, Ranganathan A, Yang X, Horton WE, Jr., Todman M, Huckle J, et al. Modification of osteoarthritis in the guinea pig with pulsed low-intensity ultrasound treatment. Osteoarthritis Cartilage. 2010;18(5):724-33.
22. Iwabuchi Y, Tanimoto K, Tanne Y, Inubushi T, Kamiya T, Kunimatsu R, et al. Effects of low-intensity pulsed ultrasound on the expression of cyclooxygenase-2 in mandibular condylar chondrocytes. J Oral Facial Pain Headache. 2014;28(3):261-8.
23. Li X, Li J, Cheng K, Lin Q, Wang D, Zhang H, et al. Effect of low-intensity pulsed ultrasound on MMP-13 and MAPKs signaling pathway in rabbit knee osteoarthritis. Cell Biochem Biophys. 2011;61(2):427-34.
24. Kusuyama J, Bandow K, Shamoto M, Kakimoto K, Ohnishi T, Matsuguchi T. Low intensity pulsed ultrasound (LIPUS) influences the multilineage differentiation of mesenchymal stem and progenitor cell lines through ROCK-Cot/Tpl2-MEK-ERK signaling pathway. J Biol Chem. 2014;289(15):10330-44.
25. Uddin SM, Qin YX. Enhancement of osteogenic differentiation and proliferation in human mesenchymal stem cells by a modified low intensity ultrasound stimulation under simulated microgravity. PLoS One. 2013;8(9):e73914.
26. Xia P, Wang X, Qu Y, Lin Q, Cheng K, Gao M, et al. TGF-beta1-induced chondrogenesis of bone marrow mesenchymal stem cells is promoted by low-intensity pulsed ultrasound through the integrin-mTOR signaling pathway. Stem Cell Res Ther. 2017;8(1):281.
27. K E, I HK, K O. Ultrasound Enhances Transforming Growth Factor Mediated Chondrocyte Differentiation of Human Mesenchymal Stem Cells. Tissue Engineering. 2004:10(5-6):921-9.
28. MA D, M D, SR Y, AJ M, J H, LA C. The significance of membrane changes in the safe and effective use of therapeutic and diagnostic ultrasound. . Phys Med Biol. 1989:34:1543–52. .
29. Chumakova OV, Liopo AV, Andreev VG, Cicenaite I, Evers BM, Chakrabarty S, et al. Composition of PLGA and PEI/DNA nanoparticles improves ultrasound-mediated gene delivery in solid tumors in vivo. Cancer Lett. 2008;261(2):215-25.
30. Zheng L, Zhang D, Zhang Y, Wen Y, Wang Y. mTOR signal transduction pathways contribute to TN-C FNIII A1 overexpression by mechanical stress in osteosarcoma cells. Mol Cells. 2014;37(2):118-25.

31. Cravero JD, Carlson CS, Im HJ, Yammani RR, Long D, Loeser RF. Increased expression of the Akt/PKB inhibitor TRB3 in osteoarthritic chondrocytes inhibits insulin-like growth factor 1-mediated cell survival and proteoglycan synthesis. Arthritis Rheum. 2009;60(2):492-500.
32. Cui X, Wang S, Cai H, Lin Y, Zheng X, Zhang B, et al. Overexpression of microRNA-634 suppresses survival and matrix synthesis of human osteoarthritis chondrocytes by targeting PIK3R1. Sci Rep. 2016;6:23117.
33. Huang Y, Wu D, Fan W. Protection of ginsenoside Rg1 on chondrocyte from IL-1beta-induced mitochondria-activated apoptosis through PI3K/Akt signaling. Mol Cell Biochem. 2014;392(1-2):249-57.
34. Jean YH, Wen ZH, Chang YC, Hsieh SP, Lin JD, Tang CC, et al. Increase in excitatory amino acid concentration and transporters expression in osteoarthritic knees of anterior cruciate ligament transected rabbits. Osteoarthritis Cartilage. 2008;16(12):1442-9.
35. Jia L, Chen J, Wang Y, Liu Y, Zhang Y, Chen W. Magnetic resonance imaging of osteophytic, chondral, and subchondral structures in a surgically-induced osteoarthritis rabbit model. PLoS One. 2014;9(12):e113707.
36. Outerbridge, Edward R, Outerbridge, K. H. The Etiology of Chondromalacia Patellae. Clin Orthop Relat Res. 2001:389:5-8.
37. Hashimoto S TK, Amiel D, Coutts RGD, Lotz M. Chondrocyte apoptosis and nitric oxide production during experimentally induced osteoarthritis. Arthritis Rheum. 1998: 41.
38. Martin JA, Brown TD, Heiner AD, Buckwalter JA. Chondrocyte senescence, joint loading and osteoarthritis. Clin Orthop Relat Res. 2004(427 Suppl):S96-103.
39. Martin JA, Brown T, Heiner A, Buckwalter JA. Post-traumatic osteoarthritisThe role of accelerated chondrocyte senescence. Biorheology. 2004:41.
40. A GR. Oxygen radicals inflammation, and arthritis: Pathophysiological considerations and implications for treatment. 1991:20(4):219-40.
41. G P, K RA, A N. How important is oxidative damage? Lessons from Alzheimer's disease. Free Radical Biology and Medicine. 2000:28(5):831-4.
42. Wang W, Cai J, Tang S, Zhang Y, Gao X, Xie L, et al. Sinomenine Attenuates Angiotensin II-Induced Autophagy via Inhibition of P47-Phox Translocation to the Membrane and Influences Reactive Oxygen Species Generation in Podocytes. Kidney Blood Press Res. 2016;41(2):158-67.
43. Circu ML, Aw TY. Reactive oxygen species, cellular redox systems, and apoptosis. Free Radic Biol Med. 2010;48(6):749-62.
44. Li J, Zhang Q, Ren C, Wu X, Zhang Y, Bai X, et al. Low-Intensity Pulsed Ultrasound Prevents the Oxidative Stress Induced Endothelial-Mesenchymal Transition in Human Aortic Endothelial Cells. Cell Physiol Biochem. 2018;45(4):1350-65.
45. Zhang K, Tu M, Gao W, Cai X, Song F, Chen Z. Hollow Prussian Blue Nanozymes Drive Neuroprotection against Ischemic Stroke via Attenuating Oxidative Stress, Counteracting Inflammation, and Suppressing Cell Apoptosis Nano Letters. 2019:19(5):2812-23.

46. Jia L, Chen J, Wang Y, Zhang Y, Chen W. Focused Low-intensity Pulsed Ultrasound Affects Extracellular Matrix Degradation via Decreasing Chondrocyte Apoptosis and Inflammatory Mediators in a Surgically Induced Osteoarthritic Rabbit Model. Ultrasound Med Biol. 2016;42(1):208-19.
47. Su Z, Xu T, Wang Y, Guo X, Tu J, Zhang D, et al. Lowintensity pulsed ultrasound promotes apoptosis and inhibits angiogenesis via p38 signalingmediated endoplasmic reticulum stress in human endothelial cells. Mol Med Rep. 2019;19(6):4645-54.
48. Suzuki N, Hanmoto T, Yano S, Furusawa Y, Ikegame M, Tabuchi Y, et al. Low-intensity pulsed ultrasound induces apoptosis in osteoclasts: Fish scales are a suitable model for the analysis of bone metabolism by ultrasound. Comp Biochem Physiol A Mol Integr Physiol. 2016;195:26-31.
49. Tianhua Xu1* JG, Chenghai Li2, Guo2 X, Tu2 J, Zhang2 D, Sun1 W, Kong1 X. Low-intensity pulsed ultrasound suppresses proliferation and promotes apoptosis via p38 MAPK signaling in rat visceral preadipocytes. AMERICAN JOURNAL OF TRANSLATIONAL RESEARCH. 2018:10(3):948-56.
50. Wang YX, Leung KC, Cheung WH, Wang HH, Shi L, Wang DF, et al. Low-intensity pulsed ultrasound increases cellular uptake of superparamagnetic iron oxide nanomaterial: results from human osteosarcoma cell line U2OS. J Magn Reson Imaging. 2010;31(6):1508-13.
51. Wu J, Liu G, Qin YX, Meng Y. Effect of low-intensity pulsed ultrasound on biocompatibility and cellular uptake of chitosan-tripolyphosphate nanoparticles. Biointerphases. 2014;9(3):031016.
52. Cheng L, Zeng G, Liu Z, Zhang B, Cui X, Zhao H, et al. Protein kinase B and extracellular signal-regulated kinase contribute to the chondroprotective effect of morroniside on osteoarthritis chondrocytes. J Cell Mol Med. 2015;19(8):1877-86.
53. Kubota E, Imamura H, Kubota T. Interleukin 1 p and Stromelysin (MMP3) Activity of Synovial Fluid as Possible Markers of Osteoarthritis in the Temporomandibular Joint Journal of Oral & Maxillofacial Surgery Official Journal of the American Association of Oral & Maxillofacial Surgeons. 1997:55(1):20-7; discussion 7-8.
54. Zheng X, Xia C, Chen Z, Huang J, Gao F, Li G, et al. Requirement of the phosphatidylinositol 3-kinase/Akt signaling pathway for the effect of nicotine on interleukin-1beta-induced chondrocyte apoptosis in a rat model of osteoarthritis. Biochem Biophys Res Commun. 2012;423(3):606-12.
55. Samad TA, Moore KA, Sapirstein A, Billet S, Allchorne A, Poole S, et al. Interleukin-1beta-mediated induction of Cox-2 in the CNS contributes to inflammatory pain hypersensitivity. Nature. 2001;410(6827):471-5.
56. D S, FQ C, Poole S ea. Tumour necrosis factor-a, interleukin-1b and interleukin-8 induce persistent mechanical nociceptor hypersensitivity. Pain. 2002:96:89-97.
57. Ahmed S, Wang N, Lalonde M, Goldberg VM, Haqqi TM. Green tea polyphenol epigallocatechin-3-gallate (EGCG) differentially inhibits interleukin-1 beta-induced expression of matrix metalloproteinase-1 and -13 in human chondrocytes. J Pharmacol Exp Ther. 2004;308(2):767-73.
58. KS M, JA M, U B, MP V, MB S, CE B. A synthetic triterpenoid selectively inhibits the induction of matrix metalloproteinases 1 and 13 by inflammatory cytokines. Arthritis Rheum 2001:44:1096–104.

59. Sekino J, Nagao M, Kato S, Sakai M, Abe K, Nakayama E, et al. Low-intensity pulsed ultrasound induces cartilage matrix synthesis and reduced MMP13 expression in chondrocytes. Biochem Biophys Res Commun. 2018;506(1):290-7.
60. Chen MH, Sun JS, Liao SY, Tai PA, Li TC, Chen MH. Low-intensity pulsed ultrasound stimulates matrix metabolism of human annulus fibrosus cells mediated by transforming growth factor beta1 and extracellular signal-regulated kinase pathway. Connect Tissue Res. 2015;56(3):219-27.
61. Ahmed S, Rahman A, Hasnain A, Goldberg VM, Haqqi TM. Phenyl N-tert-butylnitrone down-regulates interleukin-1 beta-stimulated matrix metalloproteinase-13 gene expression in human chondrocytes: suppression of c-Jun NH2-terminal kinase, p38-mitogen-activated protein kinase and activating protein-1. J Pharmacol Exp Ther. 2003;305(3):981-8.

Tables

Table 1. Macroscopic examination of the cartilage lesion grading scheme.

Grades	Macroscopic changes
0	Normal cartilage
1	Cartilage softening and/or swelling
2	Moderate fibrosis and/or local cartilage loss on cartilage surface is less than 50% of cartilage thickness
3	Severe fibrosis and/or local cartilage loss on the cartilage surface is more than 50% of the thickness of cartilage, but not exposed subchondral bone
4	Total loss of articular cartilage, exposure of subchondral bone

Table 2. Modified Mankin scoring scale.

Subgroup 1: fibrillation	1. Even surface 2. Uneven surface 3. Fibrillated and fissured within superficial zone only 4. Fissures and erosions extending below the surface zone, without extending beyond the radial zone 5. Fissures and erosions extending into the deeper zone
Subgroup 2: matrix distribution	1. Normal staining 2. Moderate loss in staining 3. Severe loss in staining 4. No staining
Subgroup 3: chondrocyte loss	1. Loss extending into a superficial zone 2. Loss extending into mid-zone 3. Loss extending into a radial zone
Subgroup 4: chondrocyte cloning	1. No clusters 2. Chondrocyte clusters in the superficial zone 3. Chondrocyte clusters in superficial to mid-zone (less than four cells) 4. Chondrocyte clusters of more than four cells located in superficial to mid-zone, or chondrocyte clusters in the deeper zone

Table 3. Cartilage lesion grades measured by macroscopic examination.

	Control	KOA	KOA+PBNPs	KOA+LIPUS	KOA+PBNPs+LIPUS
Grades	0.4±0.37	$3.4\pm0.37^{*}$	$2.7\pm0.4^{*,\#}$	$2.4\pm0.2^{*,\#}$	$1.6\pm0.2^{*,\#,\Delta,\&}$

*p<0.05 vs. Control group

#p<0.05 vs. KOA group

Δp<0.05 vs. KOA+ PBNPs group

&p<0.05 vs. KOA+LIPUS group

Table 4. Mankin scores in five groups.

	Control	KOA	KOA+PBNPs	KOA+LIPUS	KOA+PBNPs+LIPUS
Mankin score (total score)	4.66±0.09	9.99±0.42*	7.76±0.65$^{*,\#}$	7.43±0.09$^{*,\#}$	6.27±0.46$^{*,\#,\Delta,\&}$
Subgroup 1	1.17±0.05	2.41±0.09*	1.87±0.14$^{*,\#}$	1.92±0.26*	1.49±0.05$^{*,\#,\Delta}$
Subgroup 2	1.15 ±0.06	2.37±0.17*	1.87±0.08$^{*,\#}$	1.90±0.10$^{*,\#}$	1.54±0.07$^{*,\#,\Delta,\&}$
Subgroup 3	1.17±0.12	2.86±0.23*	2.05±0.47	1.78±0.08$^{*,\#}$	1.47±0.07$^{*,\#,\&}$
Subgroup 4	1.17±0.10	2.35±0.11*	1.97±0.19*	2.02±0.16*	1.77±0.38

*p<0.05 vs. Control group

#p<0.05 vs. KOA group

Δp<0.05 vs. KOA+ PBNPs group

&p<0.05 vs. KOA+LIPUS group

Figures

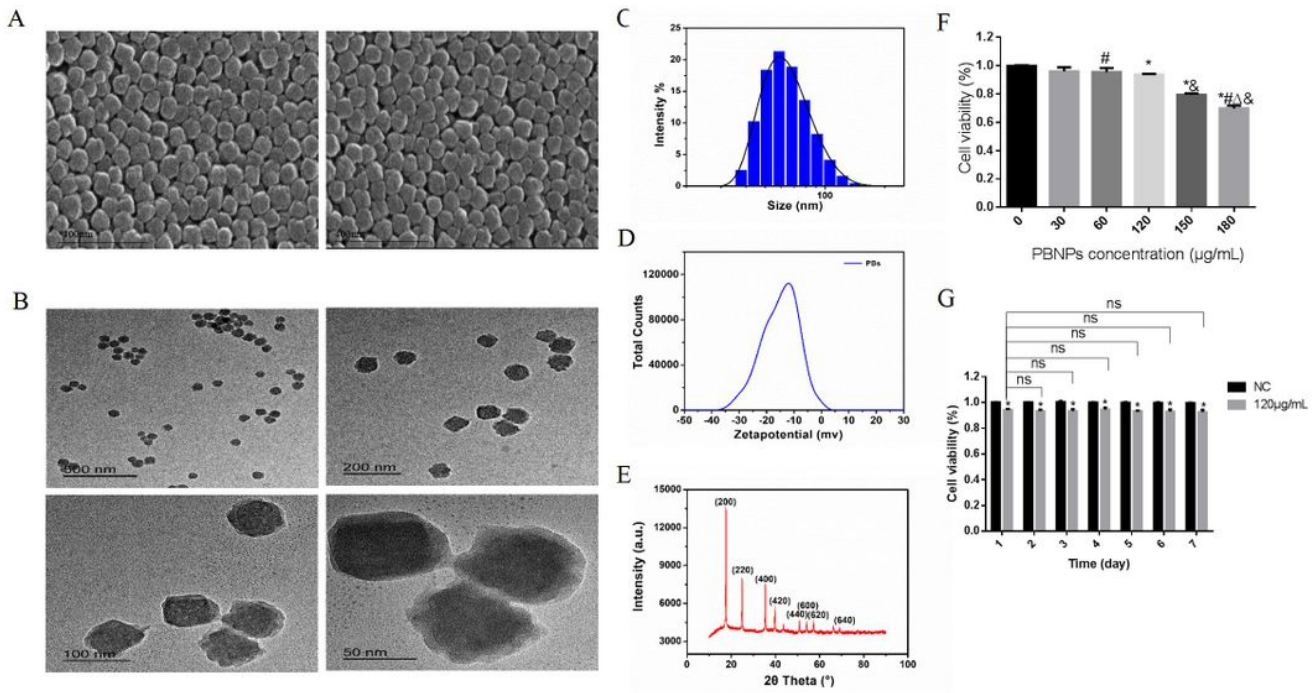

Figure 1

Characterization of PBNPs. (A) SEM image of PBNPs. (B) TEM image of PBNPs. (C) Size distribution profiles of PBNPs determined by Nano-size potentiometer. (D) Zeta potential of PBNPs. (E) X-ray diffractometer result of PBNPs. (F) Effect of various PBNPs concentrations on cells viability. (G) Effect of 120 μg/mL PBNPs on cells viability. Cells were incubated with PBNPs for 0, 1, 2, 3, 4, 5, 6, and 7 d. The statistical data were presented as the mean±SD; n=3. *p<0.05 vs. 0 μg/mL PBNPs group, #p<0.05 vs. 30 μg/mL PBNPs group, Δp<0.05 vs. 60 μg/mL PBNPs group, &p<0.05 vs. 120 μg/mL PBNPs group in Figure F.

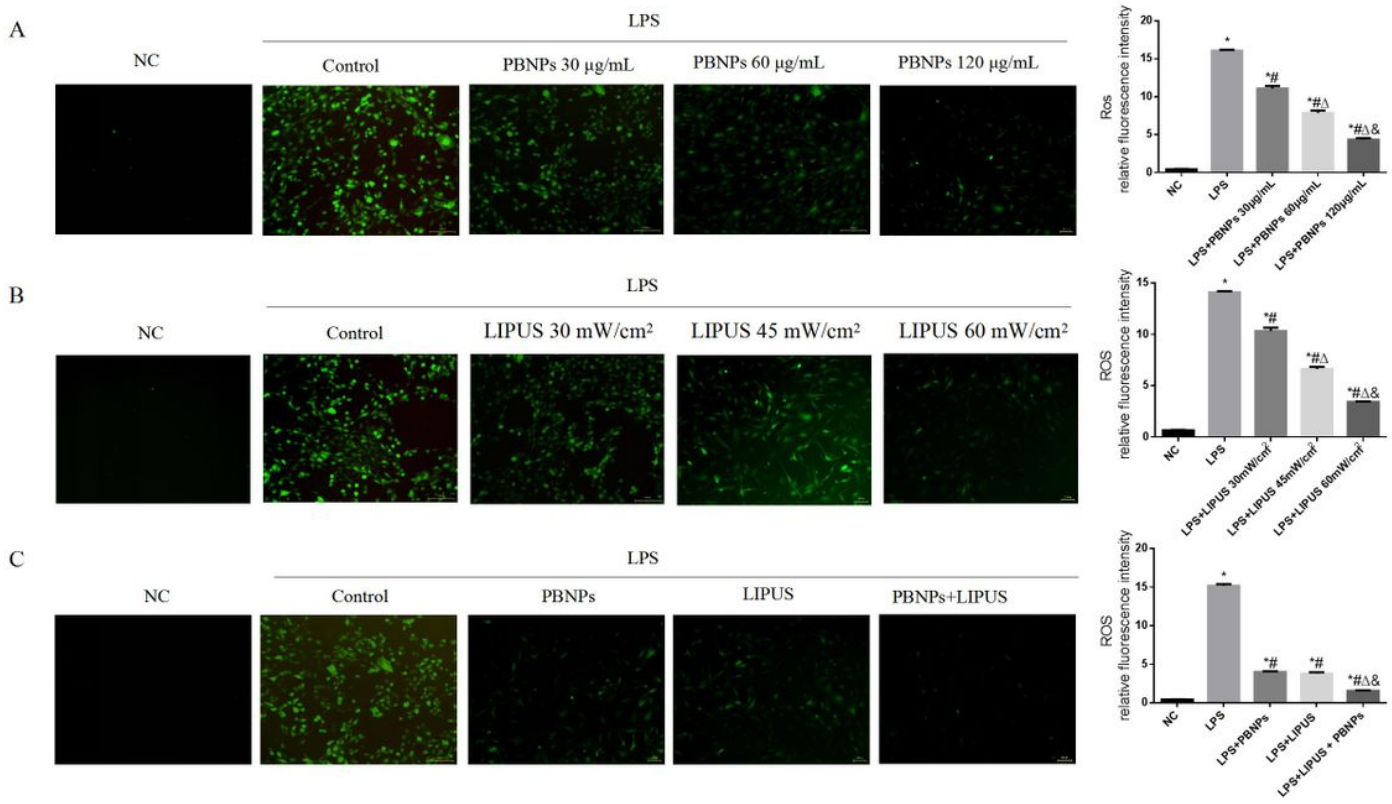

Figure 2

Effects of PBNPs/LIPUS on ROS formation in chondrocytes. Cells were pretreated with 1 μg/mL LPS for 1 h, and incubated at 30 μg/mL, 60 μg/mL, and 120 μg/mL PBNPs for 24 h as well as the various acoustic intensities (30 mW/cm2, 45 mW/cm2 and 60 mW/cm2) of LIPUS with the same other parameters (duty ratio 40 %, central frequency 1.5 MHz, repetition frequency 1 kHz and operating time 20 min per day) for 7 d in respective; 120 μg/mL PBNPs was combined with LIPUS with 60 mW/cm2 for 7 days. (A ,B, and C) Production of ROS was detected under a fluorescence microscope. The statistical data were presented as the mean±SD; n=3. *p<0.05 vs. NC group, #p<0.05 vs. LPS group in all Figures. Δp<0.05 vs. LPS+30 μg/mL PBNPs group, &p<0.05 vs. LPS+60 μg/mL PBNPs group in Figure A, Δp<0.05 vs. LPS+30 mW/cm2 LIPUS group, &p<0.05 vs. LPS+45 mW/cm2 group in Figure B, Δp<0.05 vs. LPS+PBNPs group, &p<0.05 vs. LPS+LIPUS group in Figure C.

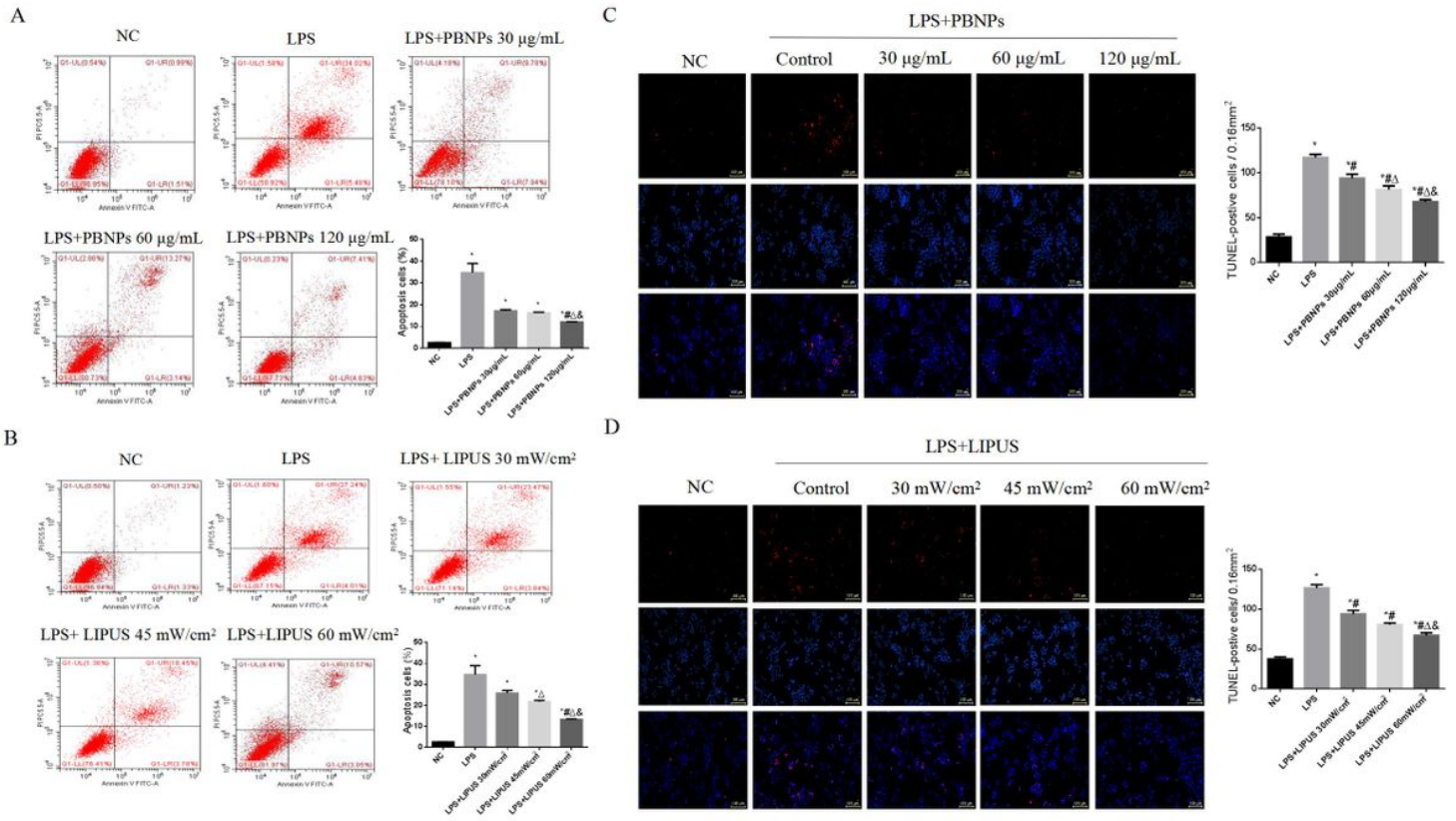

Figure 3

Effects of PBNPs and LIPUS on apoptosis in chondrocytes. Incubation was performed at different concentrations (30 μg/mL, 60 μg/mL, and 120 μg/mL) of PBNPs for 24 h and various acoustic intensities (30 mW/cm2, 45 mW/cm2 and 60 mW/cm2) of LIPUS for 7 d, cells were pretreated with 1 μg/mL LPS for 1 h. (A, B) The cell apoptosis rate was measured by flow cytometry. (C) TUNEL staining of cells. The statistical data were presented as the mean±SD; n=3. *p<0.05 vs. NC group, #p<0.05 vs. LPS group in all Figure. Δp<0.05 vs. LPS+30 μg/mL PBNPs group, &p<0.05 vs. LPS+60 μg/mL PBNPs group in Figure A and C, Δp<0.05 vs. LPS+30 mW/cm2 LIPUS group, &p<0.05 vs. LPS+45 mW/cm2 group in Figure B and D.

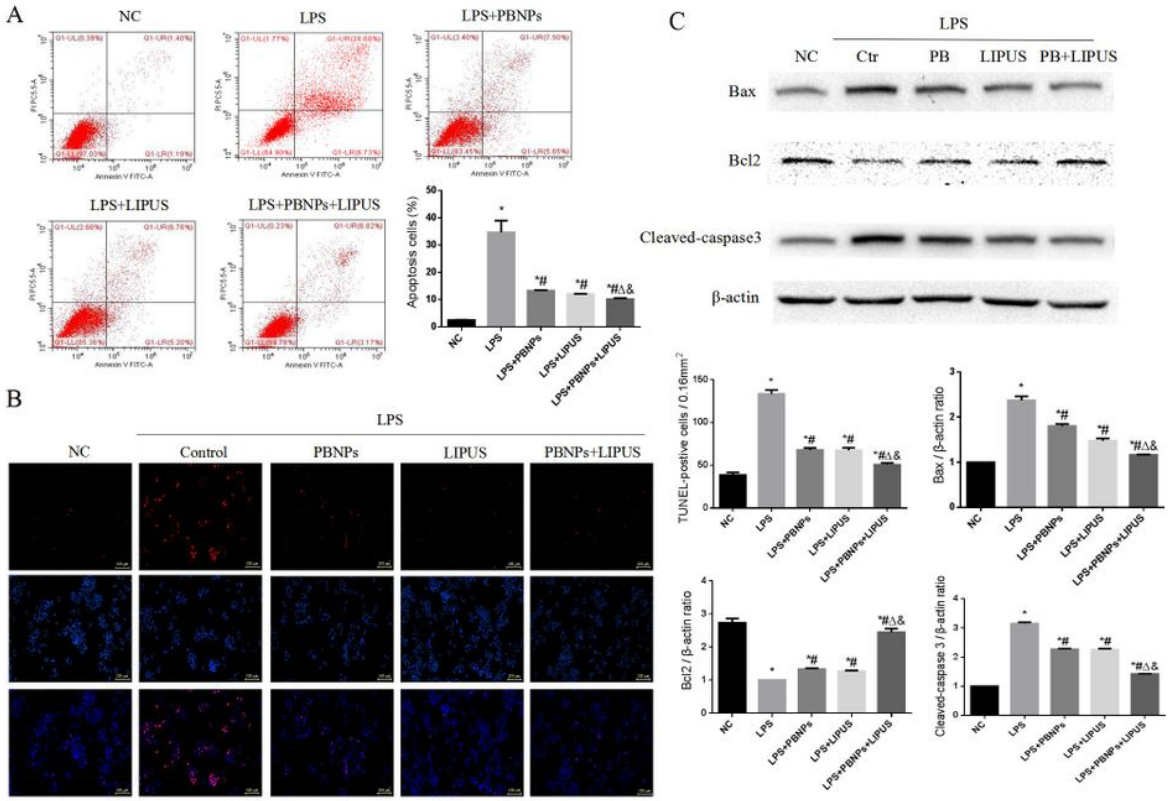

Figure 4

Effects of PBNPs combined with LIPUS treatment on apoptosis in chondrocytes. Following the incubation with 120 μg/mL of PBNPs and 60 mW/cm2 of LIPUS for 7 d, cells were pretreated with 1 μg/mL LPS for 1 h. (A) The cell apoptosis rate was measured by flow cytometry. (B) TUNEL staining of cells. (C) Representative Western blot analyses of Bax, Bcl2, and cleaved caspase-3 protein expression. The statistical data are presented as the mean±SD; n=3. *p<0.05 vs. NC group, #p<0.05 vs. LPS group, Δp<0.05 vs. LPS+ PBNPs group, &p<0.05 vs. LPS+LIPUS group.

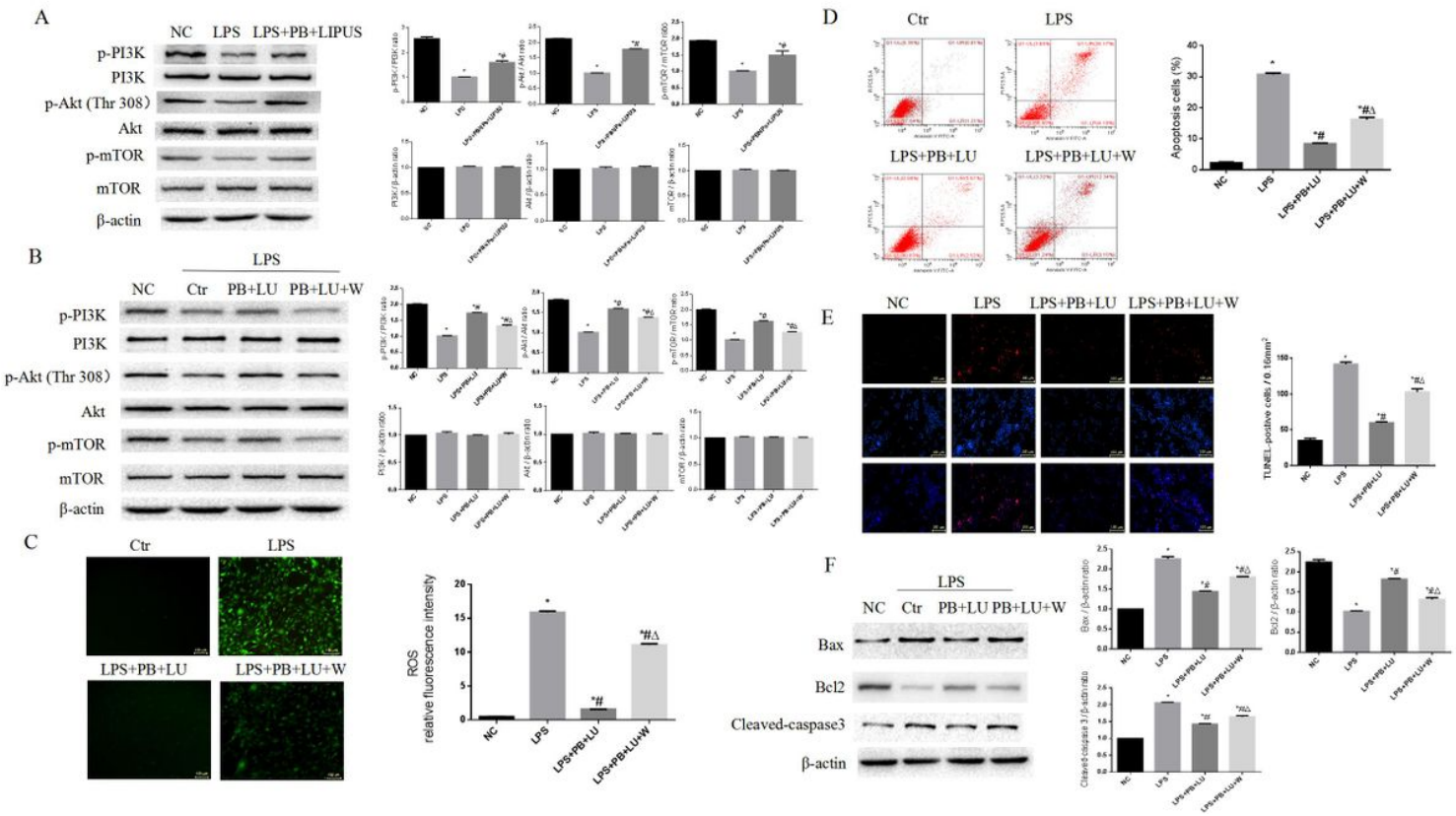

Figure 5

PBNPs/LIPUS combination treatment initiated the PI3K-Akt-mTOR pathway to reduce the LPS-induced ROS and apoptosis in chondrocytes. Following the incubation with 120 μg/mL of PBNPs and 60 mW/cm2 of LIPUS for 7 d, cells were pretreated with 1 μg/mL LPS for 1 h, and 100 nmol/L wortmannin for 2 h. (A, B) Representative western blot analyses of p-PI3K, PI3K, p-Akt (Thr308), Akt, p-mTOR, and mTOR protein expressions. (C) Production of ROS was detected under a fluorescence microscope. (D) The cell apoptosis rate was measured by flow cytometry. (E) TUNEL staining of cells. (F) Representative western blot analyses of Bax, Bcl2, and cleaved caspase-3 protein expression. The statistical data were presented as the mean±SD; n=3. *p<0.05 vs. NC group, #p<0.05 vs. LPS group, Δp<0.05 vs. LPS+ PBNPs+LIPUS group.

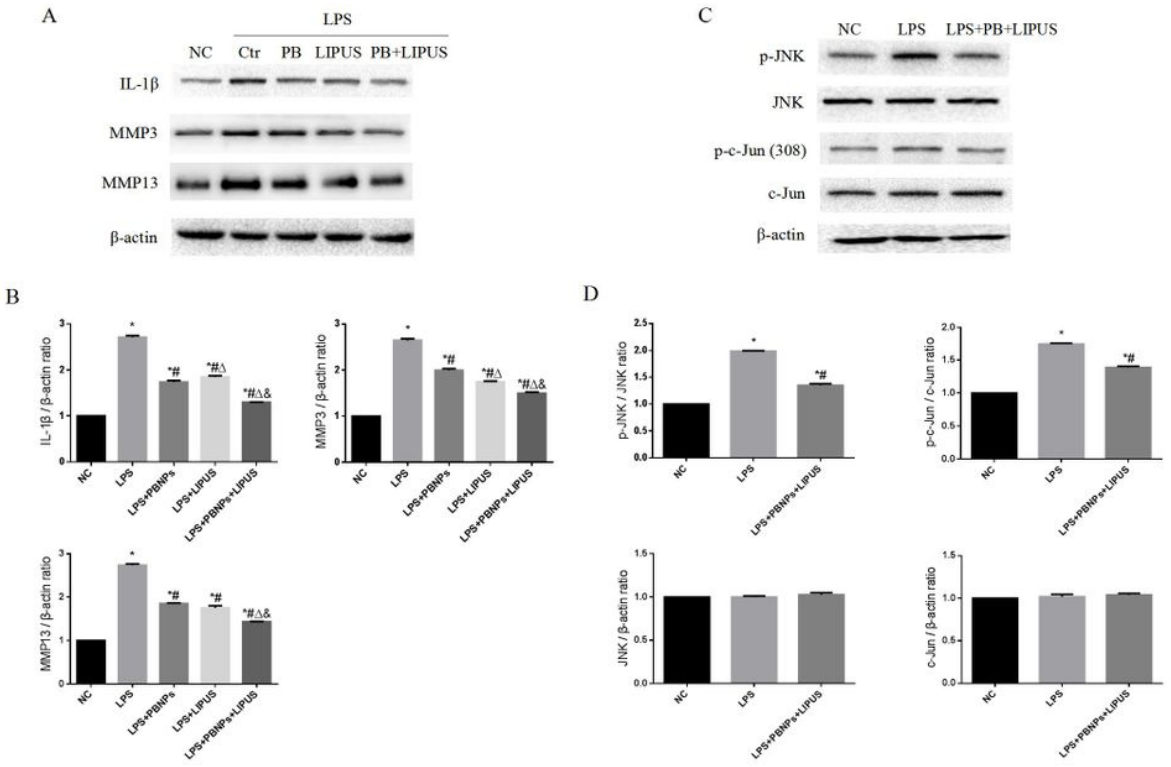

Figure 6

PBNPs/LIPUS treatment inhibited IL-1β and MMPs while activating the JINK/c-Jun signal pathway in LPS-incubated chondrocytes. Following the incubation with 120 μg/mL of PBNPs and 60 mW/cm2 of LIPUS for 7 days, cells were pretreated with 1 μg/mL LPS for 1 h. (A, B) Representative western blot analyses of IL-β, MMP3, and MMP13 protein expression. (C, D) Representative western blot analyses of p-JINK, JINK, p-c-Jun (ser308), and c-Jun protein expressions. The statistical data were presented as the mean±SD; n=3. *p<0.05 vs. NC group, #p<0.05 vs. LPS group, Δp<0.05 vs. LPS+ PBNPs group, &p<0.05 vs. LPS+LIPUS group.

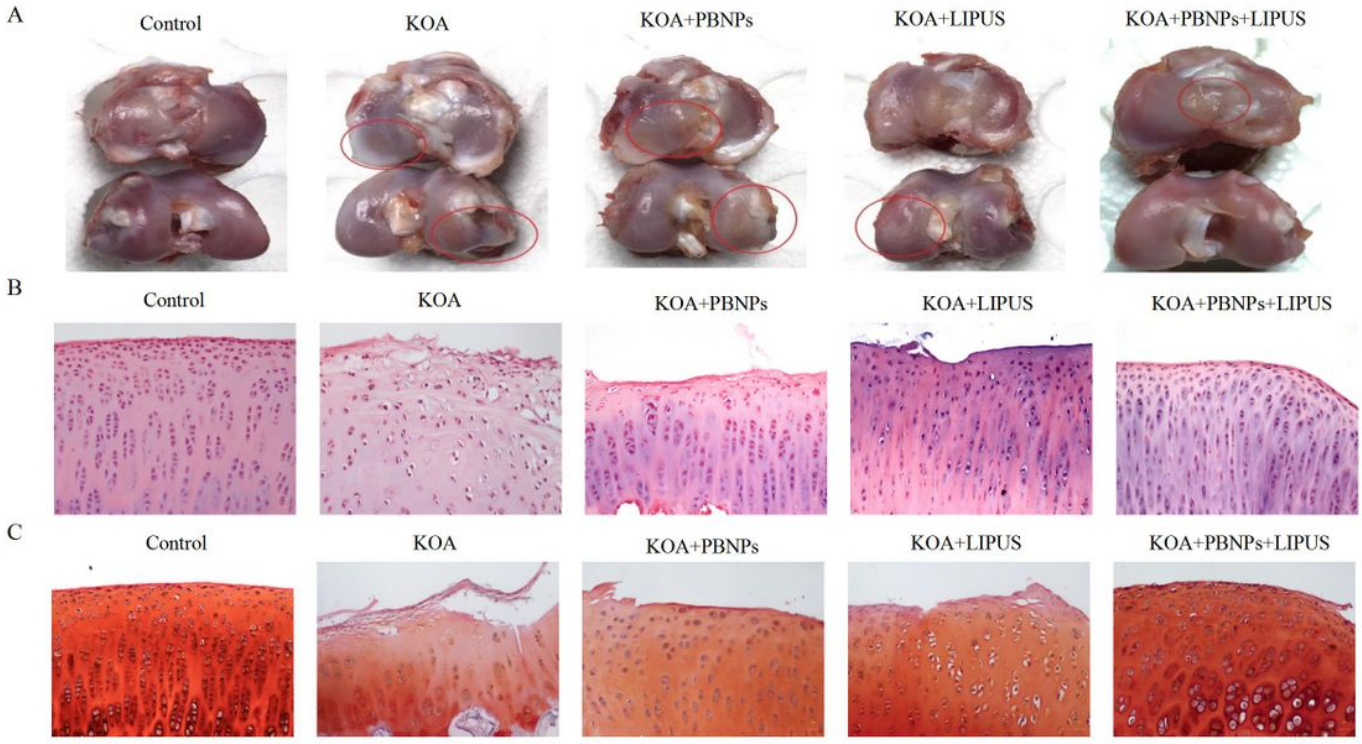

Figure 7

Effects of PBNPs/LIPUS on histopathological observations of the femoral condylar cartilage. The animals in the KOA group were subjected to the anterior cruciate ligament transection (ACLT) operation. The animals in the KOA+PBNPs group underwent ACLT with 120 μg/mL of PBNPs article injection once a wk for 6 wk. The animals in the KOA+LIPUS group were subjected to ACLT following LIPUS irradiation (acoustic intensities of 60 mW/cm2, the duty ratio of 20%, central frequency of 1.5 MHz, and repetition frequency of 1 kHz) for 20 min per d, 5 d per wk for 6 wk. The animals in the KOA+PBNPs group underwent surgery following PBNPs combined with LIPUS treatment. (A) Macroscopic observation. Circles indicated lesion areas. (B) Hematoxylin staining, ×200 magnification (n=5). (C) Safranin O staining, ×200 magnification (n=5).

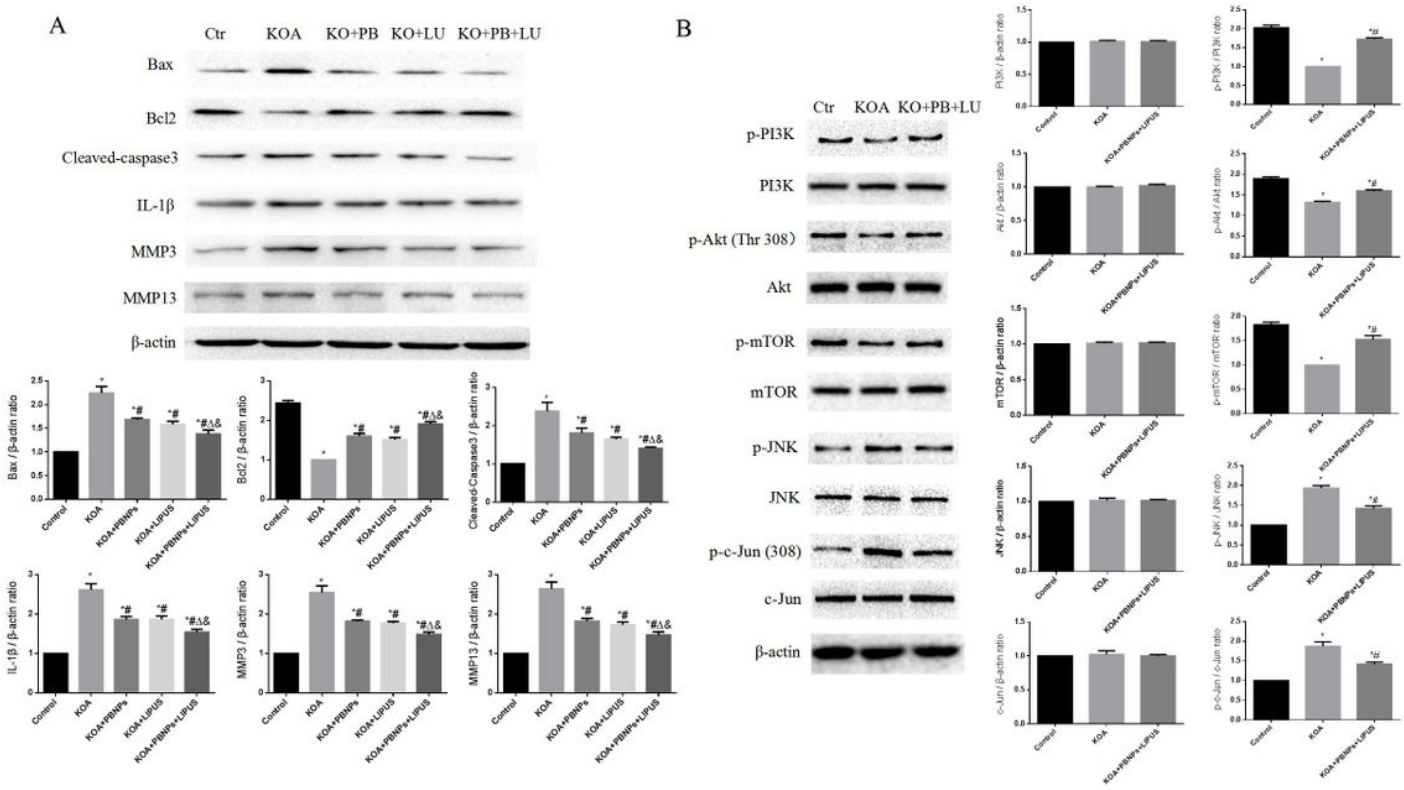

Figure 8

Effects of PBNPs/LIPUS treatment on proteins expressions of articular cartilage in rabbits with KOA. Animals of the KOA group underwent ACLT surgery. Animals of the KOA+PBNPs group underwent surgery followed by PBNPs injection. Animals of the KOA+LIPUS group underwent surgery followed by LIPUS irradiation. Animals of the KOA+PBNPs group underwent surgery following PBNPs combined with LIPUS treatment. (A) Representative western blot analyses of Bax, Bcl2, cleaved caspase-3, IL-β, MMP3, and MMP13 protein expressions. (B) Representative western blot analyses of p-PI3K, PI3K, p-Akt (Thr308), Akt, p-mTOR, mTOR, p-JINK, JINK, p-c-Jun (ser308) and c-Jun protein expressions. The statistical data were presented as the mean±SD; n=5. *p<0.05 vs. Control group, #p<0.05 vs. KOA group, Δp<0.05 vs. KOA+PBNPs group, &p<0.05 vs. KOA+LIPUS group.